

Effect of Flow Liners on Ship's Wake Simulation in a Cavitation Tunnel

Jin-Tae Lee* and Young-Gi Kim†

Abstract

Flow control devices, such as flow liners, are frequently introduced in a cavitation tunnel in order to reduce the tunnel blockage effect, when a three-dimensional wake distribution is simulated using a complete ship model or a dummy model. In order to estimate the tunnel wall effect and to evaluate the effect of flow liners on the simulated wake distribution, a surface panel method is adopted for the calculation of the flow around a ship model and flow liners installed in a rectangular test section of a cavitation tunnel.

Calculation results on the Sydney Express ship model show that the tunnel wall effect on the hull surface pressure distribution is negligible for less than 5% blockage and can be appreciable for more than 20% blockage. The flow liners accelerate the flow near the afterbody of the ship model, so that the pressure gradient there becomes more favorable and accordingly the boundary layer thickness would be reduced. Since the resulting wake distribution is assumed to resemble the full scale wake, flow liners can also be used to simulate an estimated full scale wake without modifying the ship model. Boundary layer calculation should be incorporated in order to correlate the calculated wake distribution with the measured one.

1 Introduction

Accurate simulation of a three dimensional nonuniform wake distribution is crucial for the successful model test of a marine propeller in a cavitation tunnel. In practice the simulation of a three dimensional wake distribution is not an easy task even though the same complete ship model, which was used in a towing tank, is installed in the cavitation tunnel for the simulation of the same wake distribution. Tunnel blockage effect deteriorates the flow around the ship model so that the resulting velocity field in the cavitation tunnel be different from that measured in the towing tank. The concept of employing flow liners to control the flow field near the aft-end of a ship model has been adopted by some cavitation tunnels[1].

*Korea Research Institute of Ships & Ocean Engineering, Taejon, Korea

†Samsung Heavy Ind., Taejon, Korea

Attempts to simulate the estimated full scale wake distributions by employing suitably designed flow liners were made in Ship Research Institute(SRI) of Japan. A pair of flow liners were installed in the lower corners of the tunnel wall near the aft-end of the ship. By simulating the full scale wake distributions using flow liners, better correlations between model and full scale test results were obtained not only on cavitation extents but also on pressure fluctuation values[2]. The design of flow liners, however, was carried out by a simple source method and modified by an empirical method or by a trial-and-error method[3]. A more rigorous method for the design of flow liners is needed urgently.

In this paper the effect of flow liners on the flow field around a ship model in a cavitation tunnel is studied using a surface panel method. Since the wake distribution behind a ship model is governed by the viscous effect of fluid, the assumption of ideal potential flow, on which the panel method is formulated, is not a proper one. Boundary layer correction to the calculated potential velocity distribution should be added in order to predict a reasonable wake distribution which can be correlated to the measured one. Only the relative difference between the flow around a ship model with and without flow liners is the main object of the present study.

In the previous paper by the present authors[4], the surface panel method was successfully applied to the calculation of the flow field around simple geometries, such as spheroidal bodies, in a cavitation tunnel. Calculations are extended in this paper for the Sydney Express ship model of which wake distributions were measured at the SRI cavitation tunnel with and without flow liners.

Calculation results show that the flow near the ship's aft-end is accelerated and the surface pressure gradient there becomes favorable to suppress flow separation when the flow liners are employed. It is evident from these calculations that the boundary layer thickness near the ship's aft-end would be smaller for the case of installing flow liners than that for the without-flow-liner case. Hence the width of the iso-axial velocity lines at the propeller plane when the flow liners are installed might be smaller than that for the without-flow-liner case.

2 Application of a Surface Panel Method

An irrotational flow field with the assumption of inviscid and incompressible fluid inside a cavitation tunnel, where a ship model and flow liners are installed, is solved with a low-order potential-based surface panel method [5]. A schematic drawing of the problem with the coordinate system is shown in Figure 1.

From Green's theorem, velocity potential on the ship, flow liner or wall surface can be written as :

$$-\frac{1}{2}\phi(p) = \iint_{S_S \cup S_F \cup S_W} \left[\phi(q) \frac{\partial G(p; q)}{\partial n_q} - \frac{\partial \phi(q)}{\partial n_q} G(p; q) \right] dS, \quad (1)$$

where $p(x, y, z)$ = field point where induced potential is calculated,

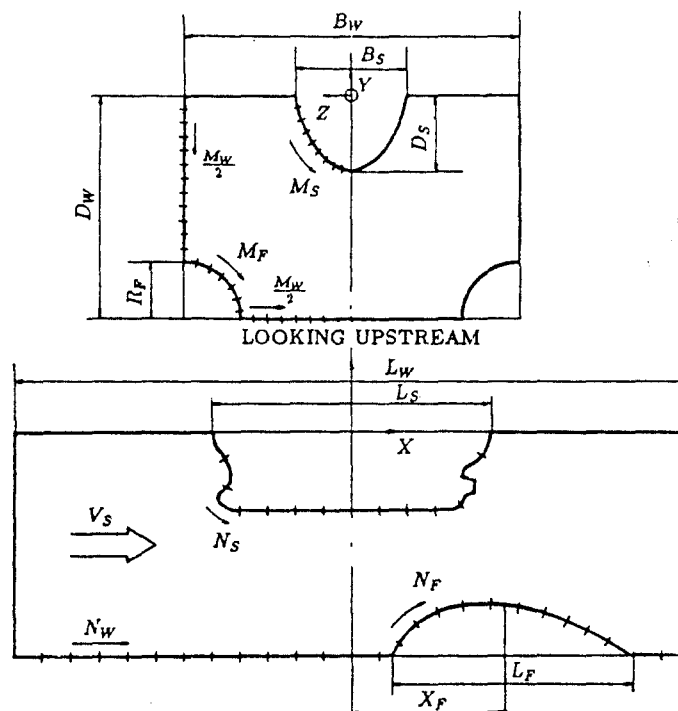


Figure 1 Arrangement of a ship model and flow liners in a cavitation tunnel.

- $q(\xi, \eta, \zeta)$ = source point where singularity is located,
- $G(p; q)$ = Green's function, $\frac{-1}{4\pi R(p; q)}$,
- $R(p; q)$ = distance between the source point and the field point,
- S_S = ship surface,
- S_F = flow liner surface,
- S_W = wall surface.

Ship, flow liner and wall surfaces are replaced by a large number of plane quadrilateral panels, where singularity strength distribution is approximated by a piecewise constant distribution over the panels.

Since the flow around the ship and flow liner is symmetric with respect to the center plane of the ship, the number of unknowns can be reduced as the half of the number of discretized panels. Instead of discretizing the tunnel upper wall surface between the ship model and the tunnel side wall, a double body ship model and a reflected side and bottom wall model is adopted to satisfy the normal boundary condition on the tunnel upper wall surface.

As shown in Figure 1, N_S panels are distributed along the longitudinal direction and M_S panels are distributed along half the cross section of a ship. The flow liner surface is replaced by $N_F \times M_F$ panels and the tunnel wall surface by $N_W \times M_W$ panels in the longitudinal and transverse direction, respectively.

Discrete form of equation (1) is

$$\sum_{j=1}^{N_P} D_{ij} \phi_j = \sum_{j=1}^{N_P} S_{ij} \left(\frac{\partial \phi}{\partial n} \right)_j, \quad i = 1, 2, \dots, N_P, \quad (2)$$

where

$$\begin{aligned} D_{ij} &= \iint_{S_j} \frac{\partial G(p_i, q)}{\partial n_q} ds, \\ S_{ij} &= \iint_{S_j} G(p_i, q) ds, \\ N_P &= \text{total number of unknowns.} \\ &(N_P = M_S \times N_S + M_W \times N_W + M_F \times N_F) \end{aligned}$$

After equation 2 is solved for ϕ_j , then the velocity is calculated by differentiating the calculated velocity potential. The surface pressure is calculated using the Bernoulli's equation. The non-dimensional pressure coefficient is defined as:

$$C_P = \frac{p - p_\infty}{\frac{1}{2} \rho V_S^2} = 1 - \left(\frac{V}{V_S} \right)^2. \quad (3)$$

3 Measured Wake Distribution of the Sydney Express Ship Model

The Sydney Express ship, a German container, has been used as a standard sample for comparative model tests of cavitation observation, hull pressure measurement and noise measurement since the 17th ITTC cavitation committee organized a comparative model test program. Detailed test conditions and test results of the full-scale experiments for the ship are given in Keller and Weitendorf[7].

Five Japanese organizations performed comparative model tests of the Sydney Express ship model for the 19th ITTC cavitation committee[1]. SRI participated in the test program. The three dimensional wake distribution in the large cavitation tunnel of SRI was simulated using the complete ship model. In order to get a better correlation between the model and full-scale test results, an estimated full-scale wake distribution was selected as a target wake to be reproduced for the cavitation tests. The estimated full-scale wake was simulated using the complete ship model and also installing a pair of flow liners in the lower corners of the tunnel side wall.

Principal dimensions of the working section of the SRI cavitation tunnel, the Sydney Express ship model and the flow liner are summarized in Table 1. Geometry of the ship model and the flow liner is shown in Figures 2.a through 2.c. Wake distribution data of the Sydney Express ship model were furnished by Dr. Ukon of SRI[6].

Figures 3 and 4 show the iso-axial velocity contour and the cross flow velocity vectors obtained from the measured wake distribution data, respectively, at the propeller plane of



Figure 2.a Surface panel representation of the Sydney Express ship model with the flow liners(side view, $N_S=20, M_S=17, N_F=20, M_F=10, N_W=20, M_W=10$).

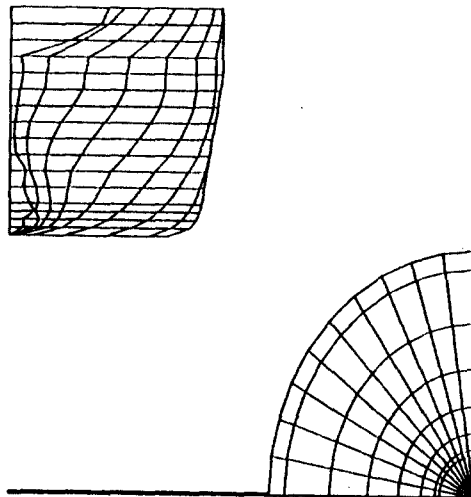


Figure 2.b sectional view, $N_S=20, M_S=17, N_F=20, M_F=10, N_W=20, M_W=10$.



Figure 2.c bottom view, $N_S=20, M_S=17, N_F=20, M_F=10, N_W=20, M_W=10$).

Table 1 Principal dimension of the working section of the SRI cavitation tunnel, the Sydney Express ship model and the flow liner.

Group	Description	Size
Tunnel working section	Length	8.0m
	Width	2.0m
	Depth	0.88m
Sydney Express ship model	Lpp	6.3m
	B	0.915m
	d(full load)	0.33m
	d(tunnel)	0.42m
Flow liner	Length	2.2m
	Max. radius	0.44m

the Sydney Express ship model without flow liner. Figures 5 and 6 show the iso-axial velocity contour and the cross flow velocity vectors for the same ship model with the flow liners, respectively.

As seen from Figures 3 and 5, width of the iso-axial velocity lines becomes narrower by employing the flow liners, which is believed to be more realistic for a full-scale ship's wake. By employing the flow liners, flow around the ship's aft-end is accelerated and the pressure gradient there becomes more favorable to suppress the development of boundary layer. The upward cross flow velocity components are increased at the upper regions between $\theta = 330$ deg and 30 deg, as shown in Figures 4 and 6.

4 Calculation of the Velocity Field around the Sydney Express Ship Model

4.1 Estimation of Tunnel Wall Blockage Effect

A low-order surface panel method is adopted for the calculation of the flow around the Sydney Express ship model with the flow liners, as described in Section 2. Surface panel representation of the ship and the flow liner is shown in Figures 2.a through 2.c, where the sizes of the ship and the flow liner and the tunnel working section is selected according to the experimental setup at the SRI cavitation tunnel.

Number of panels on the half surfaces of ship model, flow liner and tunnel wall is selected as $N_S=20, M_S=17, N_F=20, M_F=10, N_W=20, M_W=10$, respectively, so that the total number of unknowns be 740. Longitudinal length of tunnel wall is selected as three times the ship length.

After solving the boundary value problem for the unknown singularity strength distributions, the field point velocities are calculated by summing up the individual contribution from each panel and the onset velocity.

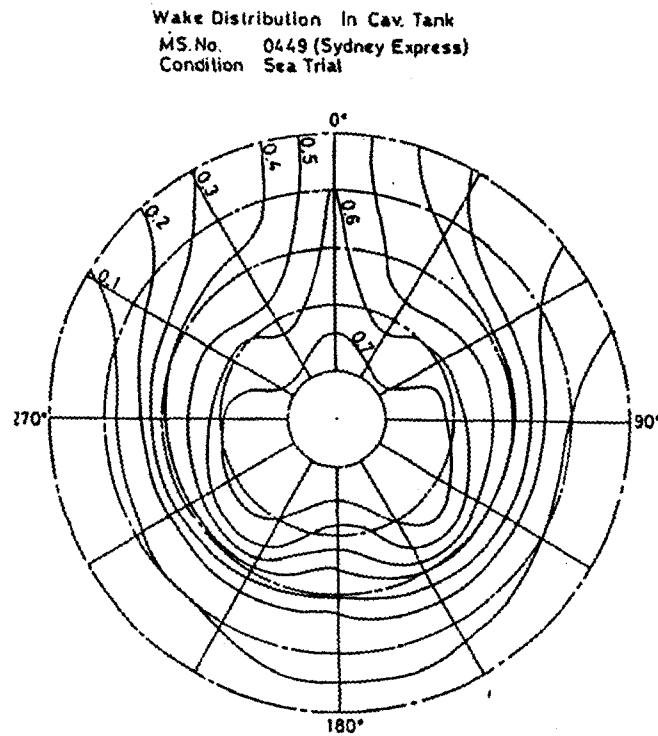


Figure 3 Iso-axial velocity contour of the measured wake distribution at the propeller plane of the Sydney Express ship model without flow liner.

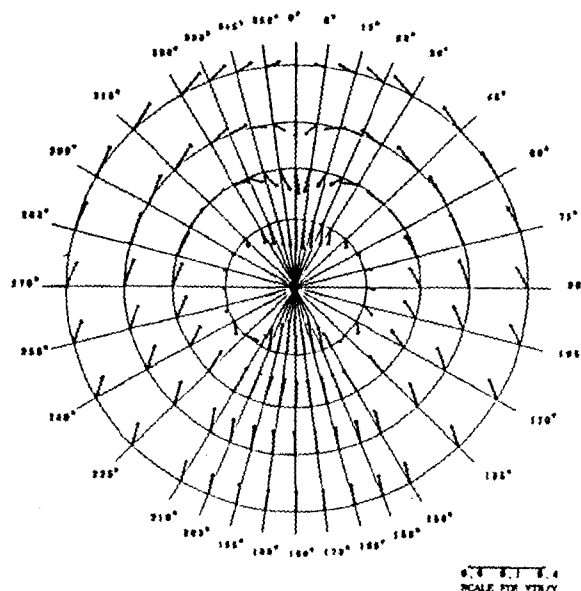


Figure 4 Transverse velocity vector plot of the measured velocity distribution at the propeller plane of the Sydney Express ship model without flow liner at radial position of $\frac{r}{R_p} = 0.381, 0.667, 0.952, 1.238$.

Estimated Wake Distribution in Cav. Tank
 MS.No. 0449 (Sydney Express)
 Condition Sea Trial

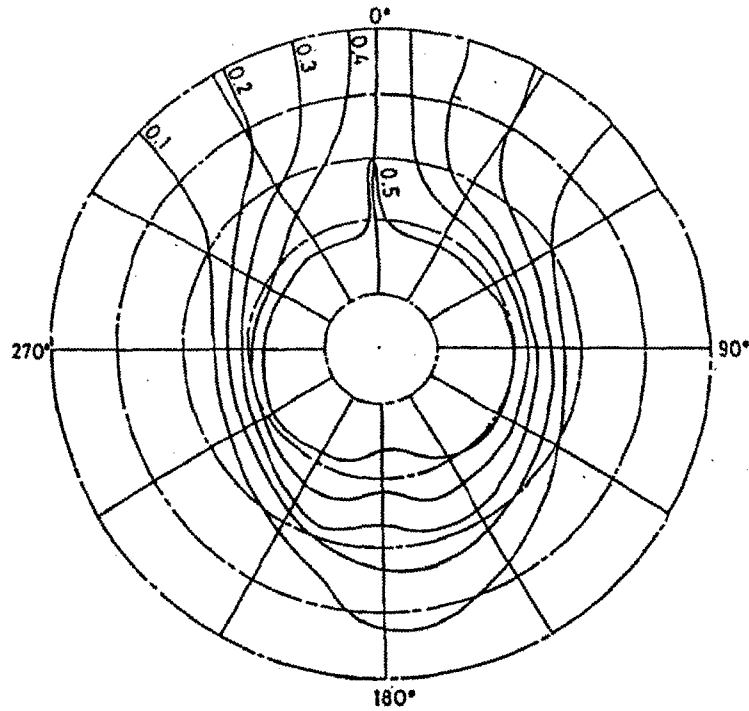


Figure 5 Iso-axial velocity contour of the measured wake distribution at the propeller plane of the Sydney Express ship model with the flow liners.

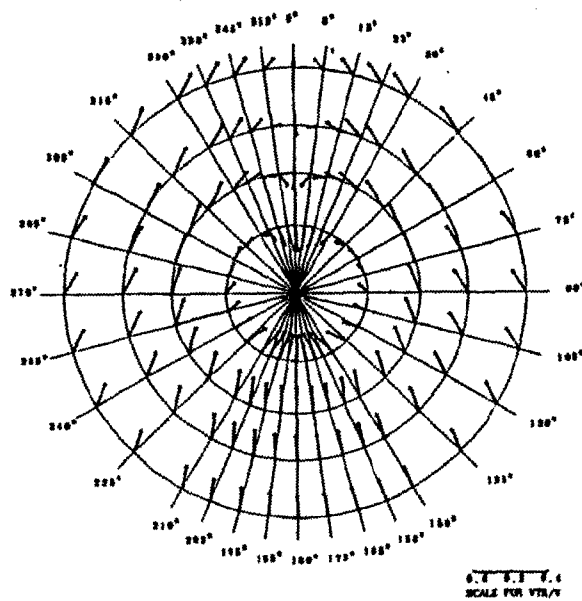


Figure 6 Transverse velocity vector plot of the measured velocity distribution at the propeller plane of the Sydney Express ship model with the flow liners at radial position of $\frac{r}{R_P} = 0.381, 0.667, 0.952, 1.238$.

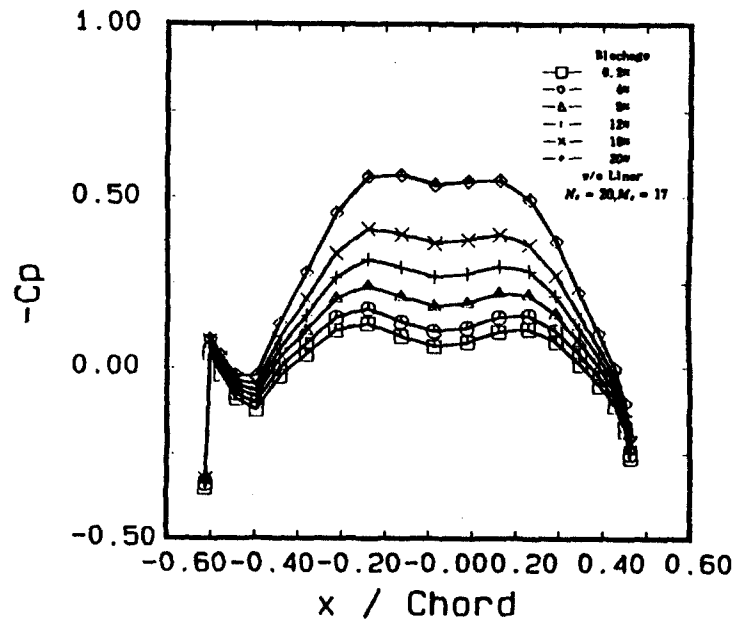


Figure 7 Pressure distributions along the longitudinal ship surface with varying tunnel wall blockages ($d/D = -0.69$, without flow liner).

In order to estimate the tunnel wall blockage effect, a series of calculations are performed for the same ship model in a rectangular test section with varying tunnel blockage. Tunnel wall blockage is reduced by increasing the sizes of tunnel wall, while keeping the same ratio of tunnel width over tunnel depth. Pressure distributions along the longitudinal ship surface above 130mm from the bottom are shown in Figure 7 for varying blockage. The tunnel blockage is defined as the ratio of the maximum ship cross section area at the midship to the tunnel cross section area.

As the blockage is increased, the pressure values at the midship decrease and the pressure gradient near the ship's aft-end becomes steeper. As the adverse pressure gradient becomes steeper near the ship's aft-end, possibility of flow separation increases. For an excessive tunnel wall blockage, the flow separates from the main stream and becomes asymmetric.

It can be stated from Figure 7 that the tunnel wall blockage effect on the ship's surface pressure distribution is negligible for the blockage less than 5% and is appreciable for the blockage more than 20% for this Sydney Express ship case. For a full ship model having high block coefficient, the flow near the ship's aft-end can be easily separated from the main stream. For these cases use of flow liner is recommended even for the case of small wall blockage.

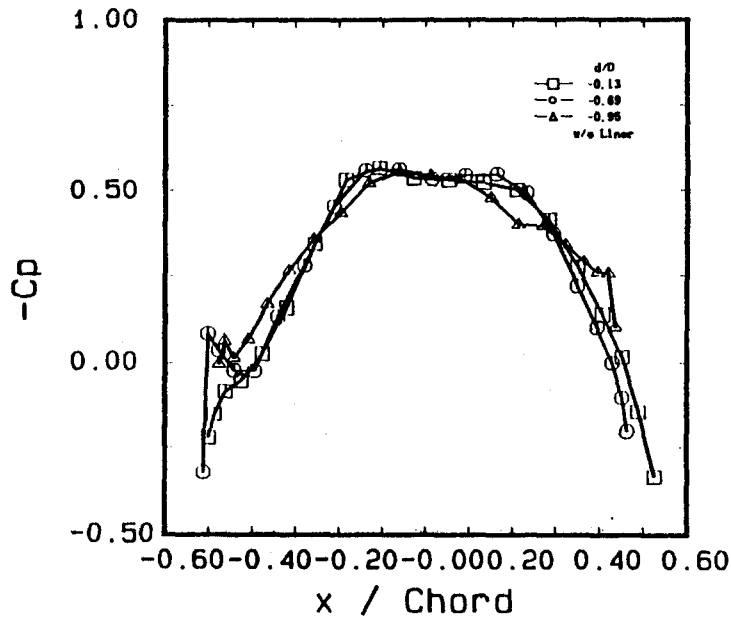


Figure 8 Pressure distributions on the ship surface calculated for the without-flow-liner case.

4.2 Flow around the Sydney Express Ship Model without Flow Liner

The pressure distributions along the three longitudinal strips of upper, middle, and bottom ship surface panels, calculated for the Sydney Express ship model without flow liner, are presented in Figure 8. The bow and stern ends, where the flow is stagnant, have higher pressure values.

The iso-axial velocity contour, generated from the calculated field point velocity distribution at the tunnel cross section of the propeller plane, is presented in Figure 9 for the without-flow-liner case. Velocities far from the ship's surface are shown to be greater than the inflow velocity to satisfy the flow continuity.

The calculated velocities on the propeller disk area are divided by the maximum value of the axial velocity on the locus of circumference of a circle having radius $\frac{r}{R_P}=1.238$, where the outermost pitot tube is located, in order to compare the calculated velocity distribution with the measured one. Here R_P designates the propeller radius. The iso-axial velocity contour and the cross flow velocity vectors at the propeller plane, reproduced from the velocity field non-dimensionalized by the maximum axial velocity, are shown in Figures 10 and 11, respectively, for the without-flow-liner case.

Since the propeller disk area is very small compared to the tunnel cross section area, the velocity differences in Figure 10 are smaller than that in Figure 9. Moreover the calculated potential velocities do not include the viscous velocity defects. Boundary correction or viscous flow calculation is needed in order to correlate the calculated velocity distribution to

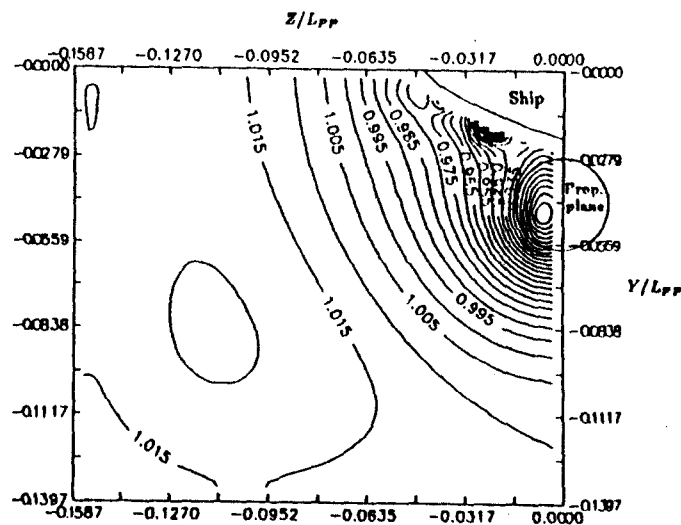


Figure 9 Iso-axial velocity contour of the field-point velocity distribution at the tunnel cross section of the propeller plane calculated for the without-flow-liner case.

the measured one. Correlation of the cross flow velocity component between the calculated and measured ones is better compared to that of the axial velocity. Exceptional regions are outer region of the angles between $\theta=330\text{deg}$ and 30deg and the inner-most region, where the influence of boundary layer of the ship surface is greater.

4.3 Flow around the Sydney Express Ship Model with Flow Liners

The pressure distributions along the three longitudinal strips of upper, middle, and bottom ship surface panels, calculated for the Sydney Express ship model with the flow liners, are presented in Figure 12. Since the flow is accelerated near the ship's aft-end due to the flow liners, pressure gradient becomes favorable up to the 85% of the ship length, while that for the without-flow-liner case is favorable only up to the 35% of the ship length from the ship's fore-end as shown in Figure 8. It can be estimated from these pressure distributions that the boundary layer thickness near the ship's aft-end would be narrower by installing the flow liners. Also the maximum pressure values at the stern end is lower for the with-flow-liner case.

The iso-axial velocity contour, generated from the calculated field point velocity distribution at the tunnel cross section of the propeller plane, is presented in Figure 13 for the with-flow-liner case. Overall flow field is seen to be accelerated appreciably due to the flow liners. The volumetric mean axial velocity on the propeller disk surface increases by 14% compared to that of the without-flow-liner case, for this Sydney Express case having 21% hull blockage and 17% flow liner blockage.

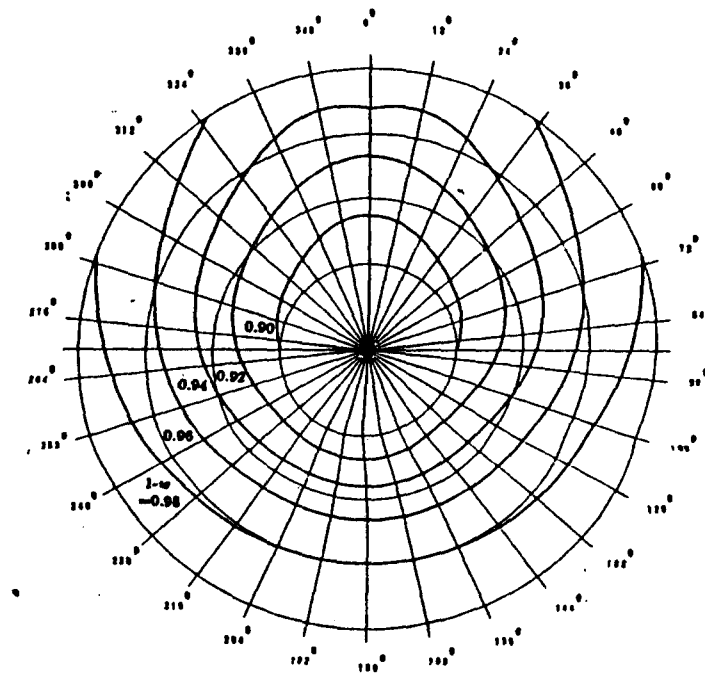


Figure 10 Iso-axial velocity contour of the non-dimensionalized velocity distribution at the propeller plane calculated for the without-flow-liner case.

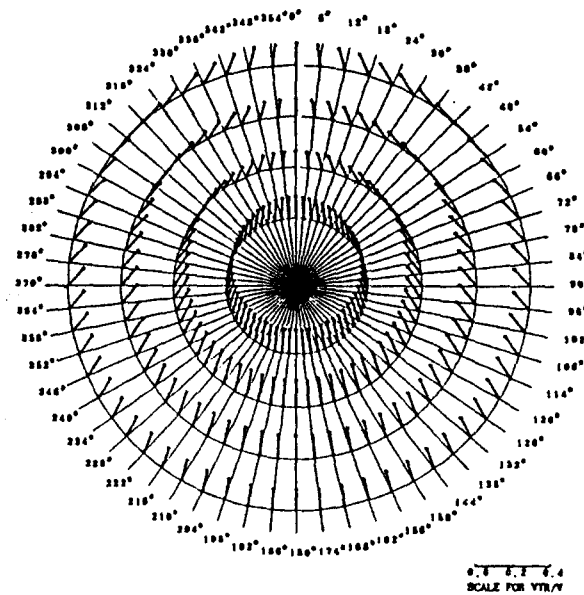


Figure 11 The non-dimensionalized transverse velocity vectors at the propeller plane calculated for the without-flow-liner case at radial position of $\frac{r}{R_P} = 0.381, 0.667, 0.952, 1.238$.

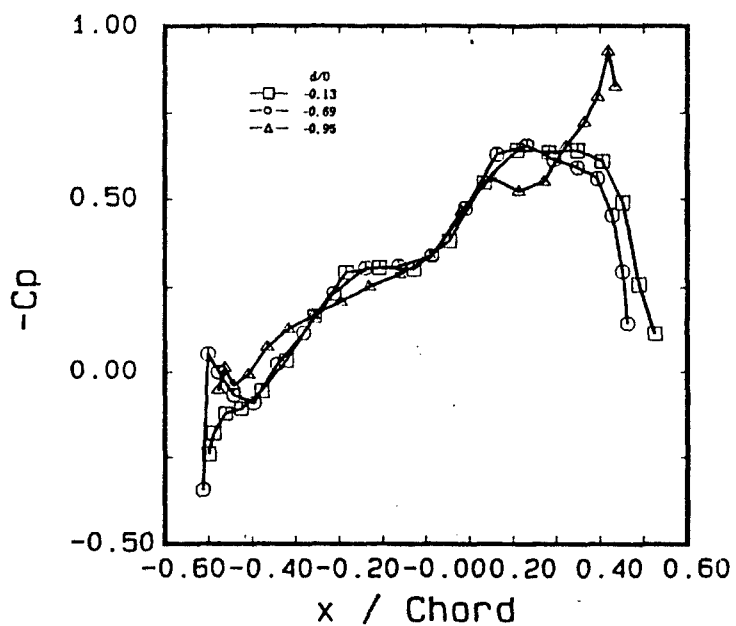


Figure 12 Pressure distributions on the ship and the flow liner surfaces calculated for the with-flow-liner case.

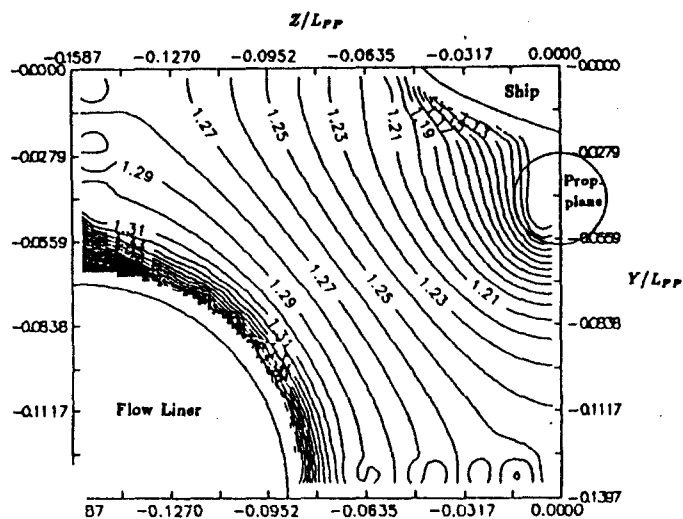


Figure 13 Iso-axial velocity contour of the field-point velocity distribution at the tunnel cross section of the propeller plane calculated for the with-flow-liner case.

The iso-axial velocity contour and the cross flow velocity vectors at the propeller plane, reproduced from the velocity field non-dimensionalized by the maximum axial velocity along the locus of circumference of the circle having radius $\frac{r}{R_P}=1.238$, are shown in Figures 14 and 15, respectively, for the with-flow-liner case. Even though overall velocities are increased appreciably by installing the flow liners, the non-dimensional iso-axial velocity contour does not change dramatically. No appreciable differences between Figure 11 and Figure 15 is found except that the upward velocity components in the outer region between $\theta=340^\circ$ and 20° are slightly increased.

5 Conclusions

In this paper a low-order surface panel method is adopted to calculate the flow around the Sydney Express ship model with flow liners in a cavitation tunnel. From the results in the previous sections following conclusions can be made :

- Velocity fields calculated at the propeller plane with and without flow liner show that flow liners can be used to control the wake distribution at the propeller plane. By designing a proper flow liner an estimated full scale target wake can be simulated in a cavitation tunnel without modifying the ship model.
- Tunnel wall blockage effect on the ship's surface pressure distribution is negligible in a close-type cavitation tunnel for the blockage less than 5% and is appreciable for the blockage more than 20% of the test section area.
- The flow liners accelerate the flow near the aft-end of the ship model so that the pressure values there be reduced. The effect of flow liners on the iso-axial velocity contour at the propeller plane, produced from the velocity field non-dimensionalized by the maximum axial velocity on the *wake-surveyed* surface, is not appreciable.
- Boundary layer correction should be added in order to correlate the calculated velocity distribution to the measured one. Since the pressure distribution near the ship's aft-end surface for the with-flow-liner case has a favorable pressure gradient to suppress flow separations, the width of the iso-axial velocity contour would become narrower compared to that for the without-flow-liner case, if the boundary layer correction is adopted.
- The CFD method solving the Navier-Stokes equations with a proper turbulent modelling is recommended for the calculation of the flow around a ship model in a cavitation tunnel with flow liners.

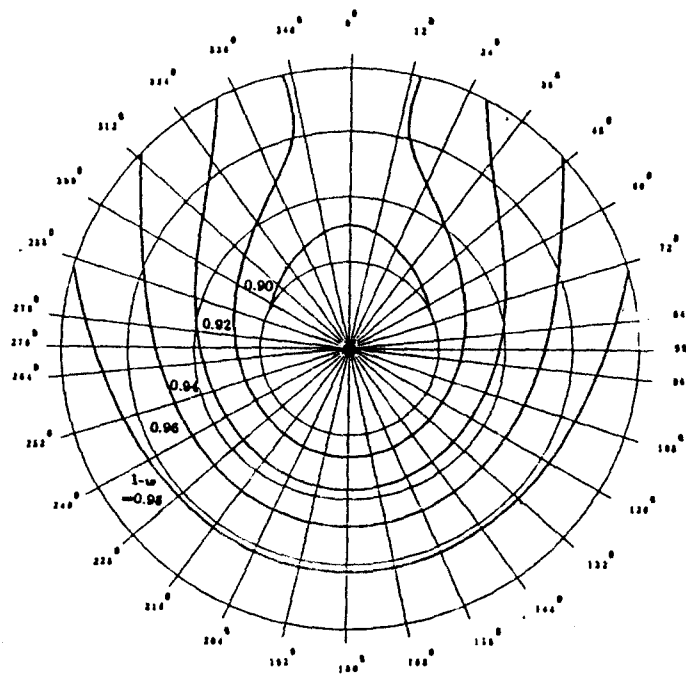


Figure 14 Iso-axial velocity contour of the non-dimensionalized velocity distribution at the propeller plane calculated for the with-flow-liner case.

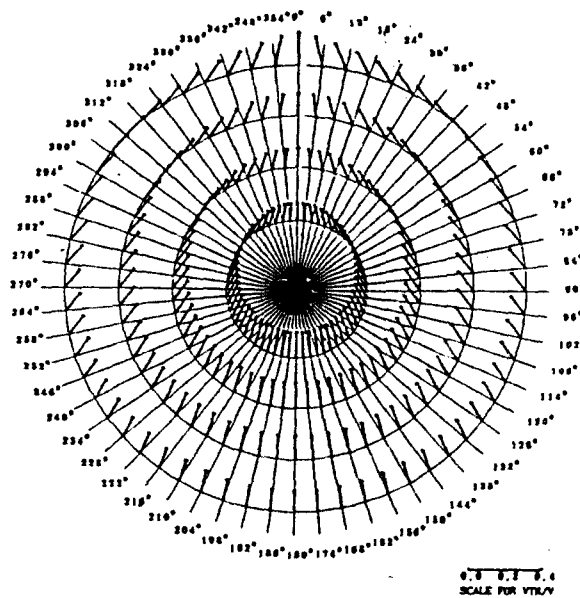


Figure 15 The non-dimensionalized transverse velocity vectors at the propeller plane calculated for the with-flow-liner-case at radial position of $\frac{r}{R_P} = 0.381, 0.667, 0.952, 1.238$.

References

- [1] ITTC, *Report of Cavitation committee*, Proc. 19th ITTC, Madrid, 1990.
- [2] Ukon, Yoshitaka, *Study on Experimental Prediction on Ship Hull Vibration Induced by Propeller and Cavitation*, Papers of SRI, Vol.28 No.4, July 1991.
- [3] Ukon, Y. and Kodama, Y., *A simple Design Method of Flow Liners*, Contribution to the 20-th ITTC, 1992.
- [4] Lee, Jin-Tae, *Calculation of the flow field around a ship model with flow liners in a cavitation tunnel*, Spring meeting of SNAK, 1992.
- [5] Lee, Jin-Tae, *A potential based panel method for the analysis of marine propellers in steady flow*, Ph.D. Thesis, Dept. of Ocean Engineering, M.I.T., 1987.
- [6] Ukon, Y., *Wake Simulation by flow liners - Sydney Express* -, Contribution to the 20-th ITTC, 1992.
- [7] Keller, A.P. and Weitendorf, E.A., *A Determination of the Free Air Content and Velocity in Front of the Sydney Express Propeller in Connection with Pressure Fluctuation Measurements*, Proc. of 12th O.N.R. Symp., Washington D.C., June 1978.